

An approximate boundary layer theory for semi-infinite cylinders of arbitrary cross-section

By E. VARLEY

Division of Applied Mathematics, Brown University, Providence

(Received 21 November 1957)

SUMMARY

An estimate is given of the distribution of skin frictional force per unit length, and of displacement area, on the outside of a semi-infinite cylinder, of arbitrary cross-section, moving steadily in a direction parallel to its generators. A Pohlhausen method is employed with a velocity distribution chosen to yield zero viscous retarding force on the boundary layer approximations. (The smallness of the fluid acceleration far from the leading edge has been pointed out by Batchelor (1954).) Like the Rayleigh method, this method is expected to yield reasonable results at large distances from the leading edge. However, for a large class of cross-sections, which includes all convex cross-sections and locally concave cross-sections with re-entrant angles greater than $\frac{1}{2}\pi$, the method yields the expected square root growth of the boundary layer at the leading-edge, with a fairly close approximation to the coefficient, and it is supposed that the skin-frictional force and displacement area are given with reasonable accuracy along the whole length of the cylinder.

Results for the elliptic cylinder and the finite flat plate are given in closed form, valid for the whole length of the cylinder, and are expected to be in error by at most 20%. In addition, some estimate is given of the effect of corners on skin frictional force and displacement area.

1. INTRODUCTION

This paper deals with the boundary layer on a long cylinder of arbitrary cross-section in a stream parallel to the generators. The shape of the nose is immaterial, but it is supposed to be smooth enough not to cause separation. It is the growth of the boundary with distance x from the leading edge, and the distribution of skin friction along the cylinder, with which this paper is concerned.

The problem for the cylinder of arbitrary cross-section has been tackled by Batchelor (1954). His work is based on Rayleigh's (1911) method of inferring a rough answer from the analogous time-dependent heat-conduction problem of determining the temperature distribution in an infinite

homogeneous solid, initially at zero temperature, but with the internal boundary (an infinitely long cylinder) maintained for $t > 0$ at a constant non-zero temperature. The time t is then interpreted as x/U , the thermal diffusivity as ν , and the temperature as the departure of the velocity u from the free stream value U .

This method assumes that vorticity in the boundary layer is convected downstream with the free stream velocity instead of the local velocity u in the boundary layer. In consequence, the boundary layer thickness is underestimated and the skin friction is overestimated.

For the cylinder of arbitrary cross-section Batchelor finds that, for small values of $\nu x/U$, the local properties in the boundary layer are independent of the cylinder cross-section. They are as in the well-known Blasius layer, for which the boundary layer thickness varies like $(\nu x/U)^{1/2}$. For the Blasius layer, Batchelor, like Rayleigh (1911), obtains for the local skin friction $0.564\mu U(\nu x/U)^{-1/2}$, when the true coefficient is 0.332. This is a serious overestimate.

At values of $\nu x/U$ for which the thickness of the boundary layer is comparable with a typical dimension l (taken to be the perimeter divided by 2π) of the cylinder cross-section, the effect of the cross-sectional shape is important. The first approximation for the effect of the shape of the cylinder on the force per unit length of cylinder is determined in terms of the number of corners and their angles in the cylinder cross-section; if there are no corners, the force on a unit length of the cylinder is the same, to this approximation, as that on a circular cylinder of the same perimeter. For large values of x/U the boundary layer thickness is large compared with l , and it is here that we expect the Rayleigh method to furnish reasonable results since conditions in a large part of the outer boundary layer approximate to free stream conditions. Batchelor shows that the bulk properties of the boundary layer for large values of x/U are the same as those for the circular cylinder which has the 'equivalent radius' c , such that the two cylinders, if given the same charge per unit length, would have the same electrostatic potential at large distances. Moreover, the rate of retardation of the fluid becomes very small.

Batchelor's solution for the general cylinder can be regarded as giving useful qualitative results, but is inadequate quantitatively except far downstream where it was shown by Glauert & Lighthill (1954) to be good.

Glauert & Lighthill (1954) investigated the boundary layer on a circular cylinder by using a Pohlhausen method with a velocity profile of the form $A(x)\log(r/c)$, where r is the distance from the axis of the circular cylinder. This profile has the virtue of satisfying conditions near the wall as accurately as possible, and of being the profile for which the viscous retarding force is identically zero. $A(x)$ was determined by substitution in the integrated momentum equation.

The results near the leading edge show good agreement with the exact solution (due to Seban & Bond (1951) and corrected by Kelly (1954)), in which the Stokes stream function is expanded in powers of $\{\nu x/(Ua^2)\}^{1/2}$.

The solution also agrees well with an asymptotic series solution, published in the same paper, which is valid far downstream.

To summarize: Batchelor has shown that for a cylinder of arbitrary cross-section far from the leading edge the viscous retarding force is very small, and in the outer part of the boundary layer where conditions are symmetrical the velocity profile is of the form $A(x)\log(r/c)$, where $A(x)$ depends upon the cylinder cross-section. Moreover Glauert & Lighthill have shown that for the case of a circular cylinder a Pohlhausen method with a velocity profile yielding zero viscous retardation gives good results along the whole length of the cylinder.

In the present paper a Pohlhausen method is again used with a velocity profile for which the viscous retarding force is identically zero along the whole length of the cylinder, and which agrees with the known solution far downstream. We expect the present method to furnish good results in the region where the boundary layer thickness is comparable with l , since in this region Batchelor shows that the viscous retarding force is small. To see whether the method, like that of Glauert & Lighthill, has value also near the nose, we expand the solutions for different shaped cross-sections at the nose and compare them with the expected Blasius solutions.

We assume the velocity profile is of the form $A(x)\phi(y, z)$, where y, z are Cartesian coordinates in the cross-sectional plane. It is further assumed that for a large distance r from an axis fixed in the cylinder boundary ϕ varies like $\log(r/c)$. The determination of ϕ is then seen to be reducible to a potential problem, the solution of which is known once we can determine the conformal mapping which transforms the exterior of the cross-section into the exterior of its 'equivalent circle', the modulus of the transformation being unity at infinity. This is the problem in electrostatics of determining the potential due to an infinite cylinder with a charge distribution of one unit of charge per unit length of the cylinder. $A(x)$ for a given cylinder is then determined from the momentum integral equation, Glauert & Lighthill's solution for a circular cylinder being a particular case.

It is shown that, only for flows down cylinders whose cross-sections contain a re-entrant angle of 90° or less, does this solution break down qualitatively at the leading edge by not giving initially the expected square-root law of boundary-layer growth with distance from the leading edge. Further for a large class of cross-sectional shapes, including circles, ellipses, convex polygons, and partly-concave polygons having re-entrant angles greater than $5\pi/8$, this method gives quantitative results at the leading edge for bulk properties, such as skin friction force per unit length, and displacement area, which are quite close to the known Blasius value, and much better than values obtained by the Rayleigh method. On the other hand, there is of course no attempt to predict velocity distributions in this or any other Pohlhausen method.

In addition, the results are expected to be good, like those given by the Rayleigh method, far downstream, because the assumption of a profile for which the viscous retarding force is zero becomes closer and closer to

the truth. Therefore, it is not unreasonable to suppose that the complete distribution of these bulk properties as functions of the distance from the leading edge is given satisfactorily.

Solutions in closed form are given for the flat plate of finite width and the elliptic cylinder. The skin frictional force and the displacement area for the flat plate are given with errors of 3% and 10% respectively at the leading edge, and for the circular cylinder errors of 13% and $\frac{1}{2}$ % in the corresponding quantities. For the general elliptic cylinder the corresponding quantities are given with errors which lie between these two sets of values. (Rayleigh's method gives an error of 70% and 35% in the skin frictional force and displacement area respectively.) It is expected that the errors gradually become less, further downstream.

The solution of the problem for the general cylinder is given in the form of a double integral which is expanded in series both at the leading edge and far downstream. These solutions can, in general, be easily joined giving a solution valid along the whole length of the cylinder. The bulk properties of the flow are seen to depend on the cross-sectional perimeter at the leading edge, and on the 'equivalent radius' far downstream, the detailed shape of the cross-section being important in the intermediate region.

Results for the finite flat plate and the square cross-section are given in tabular and graphical form. In particular, the graph of momentum defect area enables easy readings of the total frictional drag of the cylinders of any length to be made. Some consideration is also given below to several other polygonal shapes.

2. GENERAL THEORY

If u is the velocity in the x direction parallel to the generators of the cylinder whose boundary is denoted by Γ , and v, w are the velocities parallel to Cartesian axes y, z fixed in the plane of the cylinder cross-section, then the boundary layer equations for the problem of this paper are

$$u \frac{\partial u}{\partial x} + v \frac{\partial u}{\partial y} + w \frac{\partial u}{\partial z} = \nu \left(\frac{\partial^2 u}{\partial y^2} + \frac{\partial^2 u}{\partial z^2} \right) \quad (1a)$$

and

$$\frac{\partial u}{\partial x} + \frac{\partial v}{\partial y} + \frac{\partial w}{\partial z} = 0. \quad (1b)$$

Equations (1) are to be solved under the boundary conditions

$$\begin{aligned} u = v = w = 0 \quad \text{on } \Gamma, \\ u \rightarrow U \quad \text{as } x \rightarrow 0 \quad \text{or } y, z \rightarrow \infty. \end{aligned} \quad (2)$$

The method of this paper is a Pohlhausen method based upon a profile

$$u = A(x)\phi(y, z), \quad (3)$$

with ϕ chosen to yield zero viscous retarding force on the boundary layer approximations. $A(x)$ is determined for a given cylinder by substitution in the momentum integral equation

$$\rho U^2 \frac{d^{(c)}}{dx} = F, \quad (4)$$

where

$$(4) = \frac{1}{l r^2} \int_{\Sigma} u(U-u) dydz, \tag{5}$$

is the momentum defect area, Σ being the whole area outside the perimeter, and

$$F = \mu \oint_{\Gamma} \frac{\partial u}{\partial n} dr \tag{6}$$

(where dr, dn are elements of the perimeter Γ and of its outward normal) is the frictional force per unit length of the cylinder. Equation (4) may be obtained either by direct physical argument or by integrating (1 a) over the whole area outside Γ and using (1 b) to eliminate v and w .

The viscous retarding force given on the right-hand side of equation (1 a) vanishes for the profile (3) if

$$\frac{\partial^2 \phi}{\partial y^2} + \frac{\partial^2 \phi}{\partial z^2} = 0. \tag{7}$$

The particular solution of (7) with $\phi = 0$ on Γ which will be used is simply the electrostatic potential of a cylinder at zero potential and unit charge per unit length, so that

$$\int_{\Gamma} \frac{\partial \phi}{\partial n} dr = 2\pi. \tag{8}$$

The join between the profile chosen for the boundary layer and the constant value U , which u must take outside the boundary layer, is effected by writing $A(x) = U/\alpha(x)$, where $\alpha(x)$ is non-dimensional, and putting

$$\begin{aligned} u &= U \phi(y, z)/\alpha(x) & \text{for } 0 < \phi \leq \alpha, \\ u &= U & \text{for } \phi \geq \alpha. \end{aligned} \tag{9}$$

Then by (6) and (8)

$$F = 2\pi\mu A(x) = 2\pi\mu U/\alpha(x). \tag{10}$$

When ϕ has been determined, the variation of α with x follows from (4), which, with (8) and (10), gives

$$\frac{d}{dx} \int \int_{0 < \theta < z} \frac{\phi(\alpha - \phi)}{\alpha^2} dydz = \frac{2\pi\nu}{U\alpha(x)}. \tag{11}$$

Once the integral in (11) has been determined as a function of α , it is easy to obtain the relation between α and x by one further simple integration.

A seemingly objectionable feature of this method is the discontinuity in $\partial u/\partial n$ at the edge of the boundary layer (given by $\phi = \alpha$). However, Glauert & Lighthill have shown that this in itself does not lead to serious errors in a Pohlhausen treatment. Moreover, as $\nu x/(Uc^2)$ increases, the discontinuity (which is proportional to $1/\alpha$) decreases and we would expect the errors arising from it to decrease also.

It now remains to determine the integral on the left-hand side of (11) as a function of α for a given boundary shape Γ . The solution to the potential problem given by (7) and (8) has been found for a number of boundary

shapes. In particular for a circular cylinder of radius c the solution takes the form

$$\phi = \log(r/c), \quad (12)$$

and if $\zeta = re^{i\theta}$ then this can be written as

$$\zeta = ce^{\phi+i\theta} = ce^s, \quad \text{say.} \quad (13)$$

The solution of (7) and (8) for a given boundary Γ then reduces to finding the conformal mapping

$$w = f(\zeta), \quad \text{with } f(\zeta) \sim \zeta \quad \text{for large } \zeta, \quad (14)$$

which maps the exterior of the boundary Γ in the $w (= z + iy)$ plane on to the exterior of the equivalent circle of radius c in the ζ -plane. The solution of

$$w = f(ce^s) \quad (15)$$

then gives ϕ (the real part of s) as a function of y and z .

If we now change variables in (11) from the physical (y, z) -plane into the (θ, ϕ) -plane, noting that

$$dydz = |dw/ds|^2 d\theta d\phi, \quad (16)$$

the equation becomes

$$\frac{d}{dx} \int_0^\alpha \frac{\phi(\alpha - \phi)}{\alpha^2} d\phi \int_0^{2\pi} \left| \frac{dw}{ds} \right|^2 d\theta = \frac{2\nu\pi}{U\alpha}. \quad (17)$$

The mathematical problem is thus reduced to the calculation of the inner integral in (17).

A quantity of special interest is the displacement area

$$\Delta = \frac{1}{U} \iint_{\Sigma} (U - u) dydz \quad (18)$$

which represents the amount by which the fluid outside the boundary layer is displaced owing to the reduced flow inside. On the present theory (18) takes the form

$$\Delta = \int_0^\alpha \int_0^{2\pi} \frac{(\alpha - \phi)}{\alpha} \left| \frac{dw}{ds} \right|^2 d\theta d\phi, \quad (19)$$

which is a function of α . Once (17) has been solved numerically to give the variation of α with $(\nu x)/(Uc^2)$; equation (19) enables us to determine the variation of Δ with $(\nu x)/(Uc^2)$.

To check the accuracy of the method for a given cylinder we expand the solution at the leading edge in terms of the parameter $(\nu x)/(Ul^2)$ and compare it with the expected Blasius layer, where l is the perimeter divided by 2π , given in the present method by

$$l = \frac{1}{2\pi} \int_0^{2\pi} \left| \frac{dw}{ds} \right|_{\phi=0} d\theta. \quad (20)$$

3. FLAT PLATE OF FINITE WIDTH

The well-known mapping which transforms the exterior of the finite flat plate of width $4c$ in the w -plane on to the exterior of its equivalent circle

of radius c in the ζ -plane is

$$w = \zeta + c^2/\zeta, \tag{21}$$

which can be transformed by using (13) into the required form

$$w = 2c \cosh s. \tag{22}$$

The form (22) shows that this method assumes that lines of constant velocity are confocal ellipses when at the leading edge they should be flat cylinders. This is a source of error at the leading edge, although the effects may well cancel out more or less on integrating round the perimeter.

On substituting the value of $|dw/ds|^2$ given by (22) it is easily deduced that, for a flat plate of width $4c$,

$$\int_0^{2\pi} |dw/ds|^2 d\theta = 2\pi c^2(e^{2\phi} + e^{-2\phi}), \tag{23}$$

which when substituted in (17) reduces the momentum integral equation to

$$\frac{d}{dx} \int_0^\alpha \frac{\phi(\alpha - \phi)}{\alpha^2} (e^{2\phi} + e^{-2\phi}) d\phi = \frac{\nu}{Uc^2\alpha}. \tag{24}$$

The integral in (24) is

$$(1/\alpha^2)(\alpha \cosh \alpha - \sinh \alpha)\cosh \alpha,$$

whence (24) can be solved giving

$$\frac{\nu x}{Uc^2} = \frac{1}{2} \left[\cosh 2\alpha + 3 - \frac{2}{\alpha} \sinh 2\alpha + \int_0^{2\alpha} \frac{\cosh t - 1}{t} dt \right]. \tag{25}$$

The integral in (25) is a well-known exponential integral which has been copiously tabulated so that the variation of α with $(\nu x)/(Uc^2)$, and hence the skin frictional force per unit length $F = 2\pi\mu U/\alpha$, is easy to determine numerically.

For practical purposes the results are given in tabular and graphical form. The only means of finding if the solution is accurate up to the leading edge is to expand the solution in powers of $\{(\nu x)/(U^2)\}^{1/2}$ and compare the first term in the expansion for skin frictional force and displacement area with the expected exact values of Blasius. For the flat plate of finite width $4c$,

$$l = 4c/\pi. \tag{26}$$

The right-hand side of (25) may be expanded as

$$(\nu x)/(Uc^2) = \frac{1}{6}\alpha^2 + \frac{3}{20}\alpha^4 + O(\alpha^6)$$

which is easily inverted to give, using (26),

$$\frac{F}{2\pi\mu U} = \frac{1}{\alpha} = 0.321 \left(\frac{\nu x}{U^2 l^2} \right)^{-1/2} + 1.40 \left(\frac{\nu x}{U^2 l^2} \right)^{1/2} + 18.8 \left(\frac{\nu x}{U^2 l^2} \right)^{3/2} + O \left(\frac{\nu x}{U^2 l^2} \right)^{5/2}. \tag{27}$$

The exact coefficient of $\{(\nu x)/(U^2)\}^{-1/2}$ in (27) is given by Blasius as 0.332 showing that even at the leading edge the method of the present paper applied to a flat plate gives the frictional force with an error of 3%, although some cancelling of errors doubtlessly occurs. Since it is reasonable to

assume that the method becomes more accurate far downstream we see that the distribution of skin frictional force is given remarkably well along the whole length of the flat plate. In contrast the Rayleigh method gives the coefficient 0.564 which overestimates the skin frictional force by 70% at the leading edge.

$\log_{10}\left(\frac{vx}{Uc^2}\right)$	$\log_{10}\left(\frac{F}{2\pi\mu U}\right)$	$\log_{10}\left(\frac{\Theta}{2\pi c^2}\right)$	$\log_{10}\left(\frac{\Delta}{2\pi c^2}\right)$
-3.0	1.11	2.43	2.89
-2.5	0.86	2.66	1.14
-2.0	0.62	2.92	1.39
-1.5	0.39	1.17	1.63
-1.0	0.19	1.44	1.88
-0.5	0.01	1.73	0.12
0.0	1.87	0.05	0.38
0.5	1.75	0.39	0.67
1.0	1.65	0.77	0.99
1.5	1.57	1.16	1.35
2.0	1.49	1.57	1.72
2.5	1.42	1.99	2.12
3.0	1.36	2.42	2.54

Table 1. Finite flat plate.

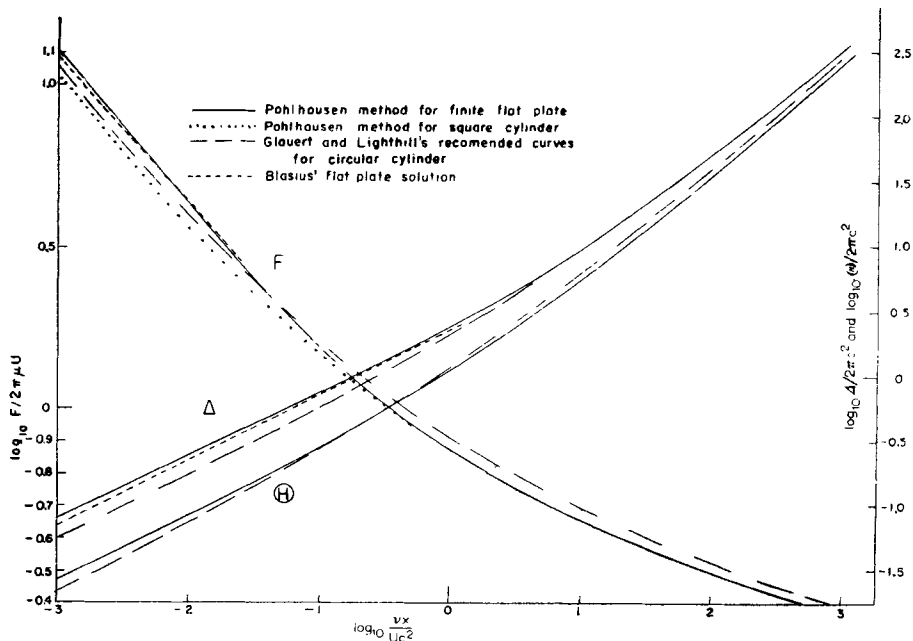


Figure 1. Frictional force F per unit length of cylinder, displacement area Δ and moment defect area Θ at distance x downstream from nose. (U = stream velocity, c = equivalent radius of cylinder.)

To determine the displacement area Δ we substitute (23) in (19) to give

$$\frac{\Delta}{2\pi c^2} = \int_0^\alpha \frac{\alpha - \phi}{\alpha} (e^{2\phi} + e^{-2\phi}) d\phi = \frac{1}{2} \frac{\cosh 2\alpha - 1}{\alpha}. \quad (28)$$

Equation (28) together with (24) enables us to find numerically the variation of Δ with x . The results are given in graphical and tabular form in table 1 and figure 1.

For conditions at the leading edge we expand the right-hand side of (28) as

$$\Delta/(2\pi c^2) = \alpha + \frac{1}{3}\alpha^3 + O(\alpha^5). \quad (29)$$

When we substitute for α in (28) as a power series in $\{(\nu x)/(U l^2)\}^{1/2}$ we obtain

$$\frac{\Delta}{2\pi l^2} = 1.924 \left(\frac{\nu x}{U l^2}\right)^{1/2} - 2.18 \left(\frac{\nu x}{U l^2}\right)^{3/2} + O\left(\frac{\nu x}{U l^2}\right)^{5/2}. \quad (30)$$

Blasius gives 1.72 as the exact coefficient of $\{(\nu x)/(U l^2)\}^{1/2}$, showing that at the leading edge the Pohlhausen method of the present paper gives an error of 11% in the displacement area. This can be compared with an error of 30% in the Rayleigh method which gives the coefficient as 1.13.

In addition to Δ , the momentum defect area $\Delta\Theta$ defined as in (5) will be considered. The integral in (5) has already been evaluated to give

$$\Theta/(2\pi c^2) = \alpha^{-2}(\alpha \cosh \alpha - \sinh \alpha) \cosh \alpha, \quad (31)$$

whence $\Theta/(2\pi c^2)$ may be plotted against $(\nu x)/(U c^2)$.

No comparison with other solutions need be made as Θ is simply proportional to the integral of the skin friction F with respect to x . The graph of Θ as a function of x gives a convenient way of determining the drag $\rho U^2 \Theta$ on a plate of length x .

4. ELLIPTIC CYLINDER

The mapping

$$w = \zeta + c^2 k/\zeta \quad (32)$$

transforms the exterior of the ellipse with axes $c(1+k)$ and $c(1-k)$ in the w -plane on to the exterior of its equivalent circle of radius c in the ζ -plane. We may assume $0 < k < 1$ since this range of k gives all possible values of the ratio of major to minor axes.

Equation (32) together with the transformation (13) gives the solution of (7) and (8) in the form

$$w = c(e^s + k e^{-s}), \quad (33)$$

from which it is easily deduced

$$\int_0^{2\pi} |dw/ds|^2 d\theta = 2\pi c^2 (e^{2\phi} + k^2 e^{-2\phi}), \quad (34)$$

and

$$l = (2c/\pi)(1+k)E[2k^{-1/2}(1+k)^{-1}] \quad (35)$$

where E is the complete elliptic integral of the second kind.

Substituting (34) in (17), the momentum integral equation becomes

$$\frac{d}{dx} \int_0^\alpha \frac{\phi(\alpha - \phi)}{\alpha^2} e^{2\phi} + k^2 e^{-2\phi} d\phi = \frac{\nu}{Uc^2}, \quad (36)$$

which is easily solved to give

$$\frac{\nu x}{Uc^2} = \frac{1}{4} \left\{ e^{2\alpha} + 3 - 4 \frac{e^{2\alpha} - 1}{2\alpha} + \int_0^{2\alpha} \frac{e^t - 1}{t} dt + k^2 \left[e^{-2\alpha} + 3 - 4 \frac{1 - e^{-2\alpha}}{2\alpha} - \int_0^{2\alpha} \frac{1 - e^{-t}}{t} dt \right] \right\}. \quad (37)$$

For conditions at the leading edge we expand the right-hand side of (37) to give

$$(\nu x)/(Uc^2) = \frac{1}{12}(1 + k^2)\alpha^2 + \frac{1}{9}(1 - k^2)\alpha^3 + \frac{3}{40}(1 + k^2)\alpha^4 + O(\alpha^5), \quad (38)$$

which is easily inverted to give together with (35), for the skin frictional force F ,

$$\frac{F}{2\pi\mu U} = \frac{1}{\alpha} = 0.455 \frac{(1 + k^2)^{1/2}}{(1 + k)E} \left(\frac{\nu x}{U^2} \right)^{-1/2} + 0.667 \frac{1 - k^2}{1 + k^2} + 0.995 \frac{(1 + k)E}{(1 + k^2)^{1/2}} \left(\frac{\nu x}{U^2} \right)^{1/2} + O\left(\frac{\nu x}{U^2} \right)^{3/2}. \quad (39)$$

The coefficient of $\{(\nu x)/(U^2)\}^{-1/2}$ is a monotonically increasing function of k and varies between 0.289 for a circular cylinder ($k = 0$) and 0.321 for a flat plate of finite width ($k = 1$). Since for any cylinder cross-section we expect the error in this method to decrease far downstream it is not unreasonable to suppose that for the case of a general elliptic cylinder the frictional force is given everywhere with an error less than 13%.

We can determine the displacement area Δ in a similar manner to that given for the flat plate and find

$$\frac{\Delta}{2\pi c^2} = \frac{1}{2} \left\{ \frac{e^{2\alpha} - 1}{2\alpha} - 1 + k^2 \left[1 - \frac{1}{2}(1 - e^{-2}) \right] \right\}. \quad (40)$$

The right-hand side of (40) can be expanded to give

$$\Delta/(2\pi c^2) = \frac{1}{2}(1 + k^2)\alpha + \frac{1}{3}(1 - k^2)\alpha^2 + O(\alpha^3), \quad (41)$$

which, with the solution of (38), gives

$$\frac{\Delta}{2\pi l^2} = 1.73 \frac{(1 + k^2)^{1/2}}{(1 + k)E} \left(\frac{\nu x}{U^2} \right)^{1/2} + O\left(\frac{\nu x}{U^2} \right)^{3/2}. \quad (42)$$

The coefficient of $\{(\nu x)/(U^2)\}^{1/2}$ is a monotonically increasing function of k and varies between 1.73 for $k = 0$ and 1.92 for $k = 1$, showing that it is not unreasonable to assume that the displacement area Δ is everywhere given with an error less than 10%.

In addition the momentum displacement area Θ is given as

$$\frac{\Theta}{2\pi c^2} = \frac{1}{4\alpha^2} [(\alpha - 1)e^{2\alpha} + (\alpha + 1) + k^2\{(\alpha + 1)e^{-2\alpha} + (\alpha - 1)\}]. \quad (43)$$

5. POLYGON CROSS-SECTIONS

We now consider the application of the present method to flow down cylinders whose cross-sections are n -sided, closed polygons with exterior angles $\pi\alpha_r$ ($r = 1, \dots, n$). Suppose that we can determine the a 's of the Schwarz-Christoffel transformation

$$dw/dt = A(t - a_1)^{\alpha_1} \dots (t - a_n)^{\alpha_n} / (1 + t^2)^2, \tag{44}$$

with

$$\sum_{r=1}^n \alpha_r = 2, \quad \sum_{r=1}^n \alpha_r / (a_r^2 + 1) = 1, \quad \sum_{r=1}^n \alpha_r a_r / (a_r^2 + 1) = 0, \tag{45}$$

which transforms the exterior of the closed polygon in the w -plane on to the lower half of the t -plane, where A is a constant and conditions (45) ensure the polygon is closed and that the solution of (44) is single-valued. Then introducing the bi-linear transformation

$$t = i(\zeta - c) / (\zeta + c), \tag{46}$$

which maps the lower half t -plane on to the exterior of the circle of radius c in the ζ -plane and which with (13) can be written

$$t = \tan(is/2), \tag{47}$$

we see that the solution of (7) and (8) reduces to solving

$$\frac{dw}{ds} = B \prod_{r=1}^n \sin^{\alpha_r} \frac{1}{2}(\theta + B_r - \phi i), \tag{48}$$

if the constant B is suitably chosen, where

$$a_r = \tan(\frac{1}{2}\beta_r) \quad (r = 1, \dots, n). \tag{49}$$

The conditions (45) become

$$\sum_{r=1}^n \alpha_r = 2, \quad \sum_{r=1}^n \alpha_r \cos \beta_r = \sum_{r=1}^n \alpha_r \sin \beta_r = 0. \tag{50}$$

From (48) it is easily deduced

$$\left| \frac{dw}{ds} \right| = B' \cosh \phi \prod_{r=1}^n \left\{ 1 - \frac{\cos(\theta + \beta_r)}{\cosh \phi} \right\}^{\alpha_r/2}. \tag{51}$$

Since we seek the solution of (55) with

$$|dw/ds| \sim ce^\phi \quad \text{for large } \phi, \tag{52}$$

we see that $B' = 2c$.

For conditions far downstream we expand

$$\int_0^{2\pi} |dw/ds|^2 d\theta \tag{53}$$

in (17) and (19) in a series valid for large ϕ which can always be written, by (50) and (51), as

$$\int_0^{2\pi} |dw/ds|^2 d\theta = 2\pi c^2 (e^{2\phi} + \sum_{m=1}^{\infty} A_m e^{-m\phi}). \tag{54}$$

If we use the form (54) the solution of the momentum integral equation giving the variation of α , and hence of frictional force, with $(\nu x)/(Uc^2)$ is

$$\frac{\nu x}{Uc^2} = \frac{1}{4} \left[e^{2\alpha} + 3 - 4 \left(\frac{e^{2\alpha} - 1}{2\alpha} \right) + \int_0^{2\alpha} \frac{e^t - 1}{t} dt \right] + \sum_{m=1}^{\infty} A_m G(\alpha, m), \tag{55}$$

where

$$G(\alpha, m) = \frac{1}{m^2} \left[e^{-m\alpha} + 3 - 4 \frac{1 - e^{-m\alpha}}{m\alpha} - \int_0^{m\alpha} \frac{1 - e^{-t}}{t} dt \right]. \quad (56)$$

In addition the variation of Δ with large α , and hence by (55) with large $(vx)/(Uc^2)$ is given in the series form

$$\Delta/2\pi c^2 = (1/4\alpha)(e^{2\alpha} - 2\alpha - 1) + \sum_1^{\infty} A_m M(\alpha, m), \quad (57)$$

where

$$M(\alpha, m) = (1/m^2\alpha)(m\alpha + e^{-m\alpha} - 1). \quad (58)$$

For conditions at the leading edge we expand (53) in a series valid for small ϕ and solve equations (17) and (19) in series valid for small $(vx)/(Uc^2)$. In particular the expected square-root behaviour in the boundary layer at the nose occurs if the integral (53) converges for $\phi = 0$.

Regular polygon

For an n -sided regular polygon it is easily shown (Bickley 1929) that

$$\beta_r = \pi r/n \quad (r = 1, \dots, n), \quad (59)$$

whence

$$|dw/ds| = 2^{\lambda} c |\sin(s/\lambda)|^{\lambda}, \quad (60)$$

where $\pi\lambda = 2\pi/n$ is the common exterior angle of the regular polygon. From (60) it is easily deduced that

$$\int_0^{2\pi} \left| \frac{dw}{ds} \right|^2 d\theta = 2^{\lambda+1} c^2 \cosh(2\phi/\lambda) \int_0^{\pi} (1 - \operatorname{sech}(2\phi/\lambda) \cos \gamma)^{\lambda} d\gamma. \quad (61)$$

The integral on the right-hand side of (61) is a hypergeometric function which can be expanded in series valid for large and small ϕ .

For conditions far downstream we expand (61) in a series valid for large ϕ , namely

$$\int_0^{2\pi} \left| \frac{dw}{ds} \right|^2 d\theta = 2\pi c^2 e^{2\phi} F_2(-\lambda, -\lambda; 1; e^{-3\phi/\lambda}), \quad (62)$$

which is in the form given by (54) and enables us together with (55) and (57) to obtain numerically the variation of frictional force and displacement area with large distance x downstream.

At the leading edge we expand (61) in the form

$$\int_0^{2\pi} \left| \frac{dw}{ds} \right|^2 d\theta = 2\pi c^2 e^{2\phi} \left[\frac{(2\lambda)!}{(\lambda!)^2} F(-\lambda, -\lambda; -2\lambda; 1 - e^{-4\phi/\lambda}) + \frac{(\lambda!)^2}{2\pi(2\lambda+1)!} \tan \pi\lambda (1 - e^{-4\phi/\lambda})^{1+2\lambda} F(1+\lambda, 1+\lambda; 2+2\lambda; 1 - e^{-4\phi/\lambda}) \right], \quad (63)$$

except for the case of a square cylinder ($\lambda = \frac{1}{2}$) when the integral on the right-hand side of (61) is an elliptic integral. The expansion of (61) given by (63) enables us to determine a series for the left-hand side of (61) valid

for small ϕ which when inserted in (17) and (19) readily gives for non-zero λ

$$\frac{F}{2\pi\mu U} = \frac{1}{\alpha} = 0.289 \left[\frac{(\lambda/2)!}{\lambda!} \right]^2 [(2\lambda)!]^{1/2} \left(\frac{\nu x}{U l^2} \right)^{-1/2} + k_1(\lambda) \left(\frac{\nu x}{U l^2} \right)^2 + k_2(\lambda) \left(\frac{\nu x}{U l^2} \right)^{1/2} + O \left(\frac{\nu x}{U l^2} \right)^{1+\epsilon}, \quad (64)$$

and

$$\frac{\Delta}{2\pi l^2} = 1.73 \left[\frac{(\lambda/2)!}{\lambda!} \right]^2 (2\lambda)! \left(\frac{\nu x}{U l^2} \right)^{1/2} + D_1(\lambda) \left(\frac{\nu x}{U l^2} \right)^{1+\lambda} + D_2(\lambda) \left(\frac{\nu x}{U l^2} \right)^{3/2} + O \left(\frac{\nu x}{U l^2} \right)^{2+\epsilon}, \quad (65)$$

where for a regular polygon

$$l = c\lambda!(\lambda/2)! \quad (66)$$

and

$$\begin{aligned} \epsilon &= \lambda, & \lambda &\leq \frac{1}{2}, \\ \epsilon &= \frac{1}{2}, & \lambda &\geq \frac{1}{2}. \end{aligned} \quad (67)$$

The coefficients of $\{(\nu x)/(U l^2)\}^{-1/2}$ in (64) and of $\{(\nu x)/(U l^2)\}^{1/2}$ in (65) vary between the limits given for a flat plate ($\lambda = 1$) and a circular cylinder ($\lambda = 0$), whence it is not unreasonable to suppose the skin frictional force per unit length and the displacement area are given everywhere with errors less than 13% and 10% respectively.

An indication is given in (64) and (65) of the effect of flow outside an angle $\pi(1 - \lambda)$ on skin frictional force and displacement area at the leading edge. For small values of λ the coefficients of the fourth terms in (64) and (65) are so large compared with the second and third coefficients that the contributions of the second and third terms are well below the level of the fourth. For values of $\lambda \sim \frac{1}{2}$ the second and third terms effectively cancel in both (63) and (64), while for values of $\lambda \sim 1$ the third terms give the effective first approximation.

The results given so far for skin frictional force agree qualitatively with a result given by Batchelor, namely: "The friction on cylinders (with inward curvature everywhere) with corners is always less than the friction on cylinders with smooth boundaries; to turn a corner sharply is more economical on drag than to do it gently with the same perimeter". The results do however disagree quantitatively with Batchelor by not predicting a finite effect for corners at the nose.

In addition a similar result holds for displacement area which can be stated: "The displacement area on cylinders (with inward curvature everywhere) with corners is always greater than the friction on cylinders with smooth boundaries; to turn a corner slowly is more economical on displacement area than to do it quickly with the same perimeter".

The values of $F/(2\pi\mu U)$ for a cylinder of square cross-section are plotted in figure 1. For $(\nu x)/(U c^2) > 1$ they are indistinguishable from those for a flat plate or circular cylinder of the same equivalent radius c . Glauert & Lighthill's recommended curve, obtained by adding 9% on to the Pohlhausen values, is probably a close approximation for all shapes in this range.

n-pronged cross

To investigate the application of the method of this paper to flows down cylinders whose cross-sections contain re-entrant angles we consider the case of the cylinder with a cross-section formed by n equal, equally spaced prongs, whence the common re-entrant angle is $2\pi/n = \pi\lambda$. The solution of (7) and (8) is such that

$$|dw/ds|^2 = 2^\lambda c |\sin(s/\lambda)]^{\lambda-1} |\cos(s/\lambda)|, \quad (68)$$

whence

$$l = 2^{\lambda+1} c / (\pi\lambda) \quad (69)$$

and

$$\int_0^{2\pi} |dw/ds|^2 d\theta = 2\pi c^2 e^{2\phi} [F(-\lambda, -\lambda; 1; e^{-4\phi/\lambda}) + 4(1-\lambda)e^{-4\phi/\lambda} F(2-\lambda, 1-\lambda; 2e^{-4\phi/\lambda})]. \quad (70)$$

The right-hand side of (70) can be written

$$2\pi c^2 e^{2\phi} \sum_{r=0}^{\infty} A_r e^{-4r\phi/\lambda}, \quad (71)$$

where

$$A_r = (\lambda-1)^2 - (\lambda-r+1)^2 (\lambda-2r)^2 / (r!)^2, \quad (72)$$

which is in the form of (54) and enables us to find the distribution of skin frictional force and displacement area far downstream.

To obtain a check on the accuracy of the method at the leading edge we continue (71) analytically for small ϕ and obtain

$$\int_0^{2\pi} \left| \frac{dw}{ds} \right|^2 d\theta = 2\pi c^2 \left[\frac{(2\lambda)!}{(\lambda!)^2 (2\lambda-1)} + B\phi^{2\lambda-1} + O(\phi^\lambda) \right]. \quad (73)$$

The right-hand side of (73) shows that only for re-entrant angles greater than 90° ($\lambda < \frac{1}{2}$) does the method of this paper yield results which are qualitatively correct at the leading edge since they give the expected square-root growth of boundary layer with distance. For re-entrant angles less or equal to 90° the surfaces of constant velocity assumed by this method at the leading edge are so different from those in reality that the momentum defect is seriously overestimated, whence the skin frictional force is overestimated. However, for re-entrant angles lying between π (flat plate) and $5\pi/8$ the skin frictional force is overestimated by between 3% and 21% while the displacement area is overestimated by between 11% and 40%. These results are better than those given by the Rayleigh method.

The greater part of this paper was written at Manchester University as a M.Sc. thesis; it was completed at Brown University under the Air Force Contract AF-49(638)-232. The author is grateful to Professor Lighthill for his helpful suggestions.

REFERENCES

- BATCHELOR, G. K. 1954 *Quart. J. Mech. Appl. Math.* **7**, 179.
 BICKLEY, W. G. 1929 *Phil. Trans. A*, **228**, 235.
 GLAUERT, M. B. & LIGHTHILL, M. J. 1955 *Proc. Roy. Soc. A*, **230**, 188.
 KELLY, H. R. 1954 *J. Aero. Sci.* **21**, 634.
 RAYLEIGH, LORD 1911 *Phil. Mag.* (6) **21**, 697.
 SEBAN, R. A. & BOND, R. 1951 *J. Aero. Sci.* **18**, 671.